Dynamics of Polymer Translocation through Nanopores: Theory Meets Experiment

Silvina Matysiak,[1] Alberto Montesi,[2] Matteo Pasquali,[1,2] Anatoly B. Kolomeisky,[1,2] and Cecilia Clementi[1,2,*]

[1]*Department of Chemistry, Computer and Information Technology Institute, 6100 Main street, Rice University, Houston, Texas 77005, USA*

[2]*Department of Chemical and Biomolecular Engineering, Computer and Information Technology Institute, 6100 Main street, Rice University, Houston, Texas 77005, USA*

(Received 5 October 2005; published 22 March 2006)

The dynamics of translocation of polymer molecules through nanopores is investigated via molecular dynamics. We find that an off-lattice minimalist model of the system is sufficient to reproduce quantitatively all the experimentally observed trends and scaling behavior. Specifically, simulations show (i) two translocation regimes depending on the ratio of pore and polymer length, (ii) two different regimes for the probability of translocation depending on applied voltage, (iii) an exponential dependence of translocation velocity upon applied voltage, and (iv) an exponential decrease of the translocation time with temperature. We also propose a simple theoretical explanation of each of the observed trends within a free energy landscape framework.

DOI: 10.1103/PhysRevLett.96.118103 PACS numbers: 87.15.La, 87.15.Aa

The translocation of a polymer molecule through a highly confined geometry is relevant in both chemical and biological processes [1–3]. Many experiments have been performed in recent years on single-stranded DNA and RNA molecules driven through an α-hemolysin membrane channel via electrophoresis; the translocation time and probability have been measured over a wide range of conditions [1,4–13]. DNA and RNA translocation is important in the characterization of viral injection and in the design of sequencing techniques; thus, understanding this phenomenon may lead to new and improved biotechnological applications. Because of the universality of polymer behavior, DNA experiments should yield generalizable results on the dependence of the dynamics of translocation on the physical parameter for generic linear macromolecules. In such a ''polymer physics'' perspective, the chemical details of the DNA and RNA chains and of the pore are less relevant; thus, coarse-grained computational models can provide insight and bridge experimental results and theoretical understanding. Many simplified computational and theoretical approaches have been proposed [14–24]; however, a simple model that can recover all the key experimental results is still missing.

In this Letter we propose a coarse-grained model for the polymer chain and the nanopore. The model reproduces quantitatively all the trends and scaling laws observed in experiments by introducing three free parameters which are fit to experimental data. Moreover, we interpret the results within a theoretical framework [20] and explain all the experimental results and relate them to relevant phenomenological parameters. The present work is a step forward towards the understanding of polymer translocation through nanopores and lays a base for further modeling, which might include chemical and physical details of the pore and polymer. Such model improvements may yield *ab initio* predictions of the free parameters.

The linear polymer molecule (Fig. 1) is represented as a semiflexible chain of N beads, with contour length $l = Na$, where a is the bead-bead equilibrium distance. A single nanopore is considered as a structureless cylindrical tube of length $L = 12a$ and diameter $D = 3.75a$ in agreement with the dimensions of the narrowest part of the α-hemolysin membrane channel [1]. The potential energy of the system is

$$U = \sum_{i=1}^{N} k_r (r_{i,i+1} - a)^2 + \sum_{i=2}^{N} k_\theta (\theta_{i-1,i,i+1} - \theta_0)^2 + \epsilon_p \sum_{i \le j-4} \left(\frac{\sigma_p}{r_{ij}}\right)^{12} + \sum_i q_i V_{\mathrm{el}}(r_i) + 4\epsilon_{\mathrm{LJ}} \sum_i \left[\left(\frac{\sigma_{LJ}}{r_{i,\mathrm{wall}}}\right)^{12} - \left(\frac{\sigma_{LJ}}{r_{i,\mathrm{wall}}}\right)^{6}\right] \quad (1)$$

where the first two terms are the harmonic bond potential and the bending potential, respectively, the third term is the excluded volume, the fourth term is the potential energy of

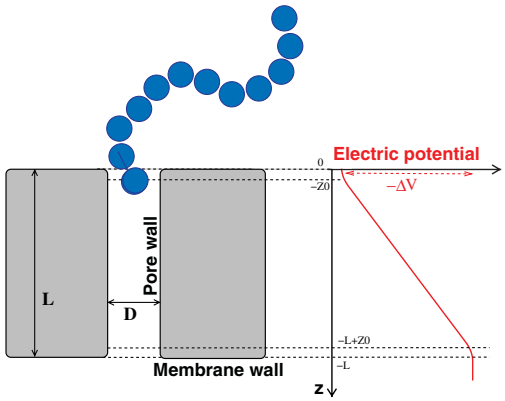

FIG. 1 (color). Schematic representation of the simulation model for polymer and nanopore.

the polymer in the external electric field, and the last term accounts for the van der Waals interaction between the polymer and the pore or membrane walls (see caption of Fig. 2 for the definition of all the constants). The electric field increases linearly across the pore, and is smoothed at the entrance and at the exit of the pore to avoid any discontinuities in the forces (Fig. 1). We use the package AMBER6 [25] (properly modified to include the effects of nanopore and electric field) to perform molecular dynamics simulations at constant temperature with implicit solvent [26]. The dynamics is described by a Langevin equation including the coupling with the thermal bath [26]:

$$m\ddot{\mathbf{r}}_i = -\frac{\partial U}{\partial \mathbf{r}_i} + \frac{m}{2\tau_0}\left(\frac{T_0}{T} - 1\right)\dot{\mathbf{r}}_i\,. \qquad (2)$$

We perform hundreds of realizations of the translocation event for each set of simulation conditions. In each initial configuration one end of the polymer is placed at the pore entrance (Fig. 1), whereas the positions of the remaining beads are sampled randomly from the equilibrium distribution of the free polymer. The simulation conditions are defined through three effective parameters—strength of the pore-polymer attraction ϵ_{LJ}, unit charge q, and coupling time constant τ_0 (or, equivalently, hydrodynamic friction coefficient ξ [26])—and two external parameters—applied voltage V and temperature T. All the other terms in Eq. (1) are polymer properties that can be evaluated from known data (see Fig. 2). The parameter τ_0 regulates the time scale of the simulations; the three energy scales of the system are RT, qV, and ϵ_{LJ}. In dimensionless terms, two energy ratios are relevant, e.g., $qV/\epsilon_{\mathrm{LJ}}$ and $RT/\epsilon_{\mathrm{LJ}}$. Each of the intrinsic parameters is estimated by comparing iteratively simulations and experimental results. τ_0 is evaluated by comparing results at different polymer length and fixed temperature and voltage. The parameter τ_0 is then held fixed to the value so determined and q is obtained by varying V while keeping temperature and polymer length fixed. Finally, simulations at different temperatures at fixed L and V (and fixed values of τ_0 and q) yield ϵ_{LJ}.

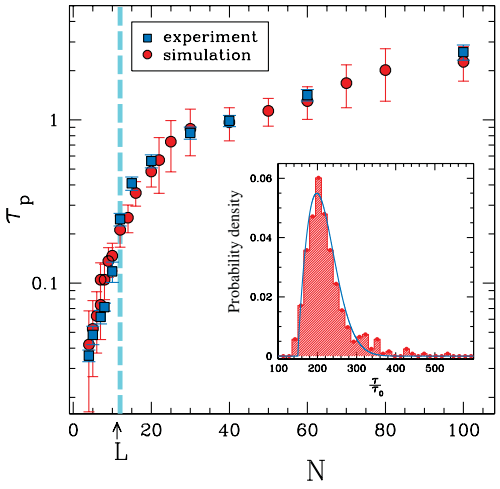

FIG. 2 (color). Translocation time vs polymer length: comparison between simulation and experimental results poly(dA) [7,12]. Inset: distribution of translocation times. For all the simulation results shown, the monomer size is $a = 4$ Å, monomer mass $m = 312$ amu, elastic constant between monomers $k_r = 2736\epsilon_{\mathrm{LJ}}/a^2$, bending stiffness $k_\theta = 8\epsilon_{\mathrm{LJ}}$ [18,24], equilibrium angle between successive connectors $\theta_0 = \pi$, Lennard-Jones parameters $\epsilon_p = 0.54$ kcal/mol, and $\sigma_{\mathrm{LJ}} = \sigma_p = a$ [28]. The three effective parameters ϵ_{LJ} (regulating the pore-polymer stickiness), q (the charge per monomer), and τ_0 (the coupling time constant, related to the hydrodynamic friction coefficient ξ) are extracted from the comparison of simulation and experimental data, as detailed in the text.

Two different regimes of translocation dynamics have been observed in experiments where the polymer length is varied: molecules shorter than the pore length move much faster than molecules longer than the pore. These two regimes have been predicted theoretically using a simple free energy landscape argument [20]. Essentially, the existence of these two regimes is mainly ascribable to the free energy contribution corresponding to the configurational entropy associated with the polymer ends hanging out of the pore: this entropy is significant only for polymers longer than the pore.

Our simulation results (Fig. 2) agree with both theory and experiment and confirm the existence of two different translocation regimes depending on the ratio l/L of polymer and nanopore length: when $l/L \leq 1$, the velocity inside the pore drops with growing l, whereas when $l/L > 1$ the polymer moves at constant speed and the translocation time grows linearly with polymer length. The simulation and experimental data fully agree within the error bars once the effective parameter τ_0 is properly adjusted; values for the friction coefficient in the range $[7 \times 10^{-9}, 1.4 \times 10^{-8}]$ kg s^{-1} give a $\chi^2 < 1.0$, with an optimal value $\xi_{\mathrm{opt}} \approx 10^{-8}$ kg s^{-1}. This is consistent with both experimental and theoretical estimates [15,20]. The simulations reproduce correctly the asymmetric fat-tailed distribution of translocation times, which is captured well by a Weibull distribution (Fig. 2, inset) over the whole range of parameters investigated (see also Ref. [18]). Because the distribution is positively skewed, the average translocation time is larger and less significant than the most probable translocation time—the latter is reported here, as commonly done in experimental reports. Consistently with experimental results, the standard deviation of the time distribution of the shorter chains is much larger than that of the longer ones. Clearly, pore-polymer interactions and polymer conformation at the pore entrance are far more important for shorter chains, and this accounts for the larger scatter of translocation times.

Figures 3 and 4 show that the simulations reproduce quantitatively the experimentally measured dependence of translocation probability and translocation time on the applied voltage. Specifically, the simulations clearly show two different regimes for the translocation probability P depending on the voltage V (Fig. 3). P is computed as the

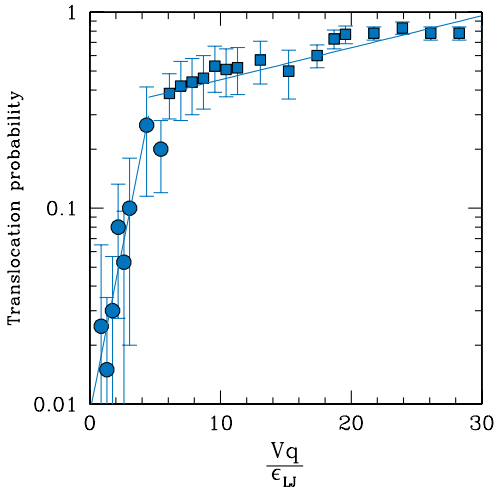

FIG. 3 (color). Effect of applied voltage on translocation probability. The different symbols corresponds to the different identified regimes.

fraction of simulations leading to a successful translocation at given conditions. Experimental results [12] show that the capture rate as a function of applied voltage exhibits two regimes. Both regimes are well approximated by exponential fits (Fig. 3), in agreement with a previous theoretical estimate [20]. The translocation probability computed in our simulations is qualitatively comparable to the capture rate measured in experiments (defined as the inverse of the time lag between two capture events); a more quantitative comparison of the data is not possible as the capture rate depends also on the polymer concentration.

Figure 3 shows that at low voltage the translocation probability increases steeply with the applied voltage, while it slowly approaches saturation at high voltage. This change of scaling behavior can be explained in terms of change in translocation mechanism from "barrier crossing" to "downhill." The two regimes, barrier crossing and downhill, are very different, and this translates into a clear change of the trend of $\ln P$ vs V. For a fixed polymer length and temperature, as the applied potential is increased the regime is a barrier-crossing one until the barrier completely disappears where $V = V_{\text{crossover}}$; upon further increase the process becomes downhill. If the applied voltage is smaller than the free energy barrier associated with the translocation process, the translocation mechanism can be considered as a diffusion over a free energy barrier. Increasing the applied voltage reduces the effective barrier, and therefore significantly increases the probability of translocation. On the other hand, when the applied voltage is comparable to the free energy barrier associated with the translocation, the process becomes essentially downhill. Clearly, increasing the applied voltage in the downhill regime does not significantly affect the probability of translocation, as the probability is already close to 1. For a fixed applied voltage, the free energy barrier becomes larger as the polymer length and temperature are increased. Thus, the change in regime $V_{\text{crossover}}$ depends on the polymer length and the temperature. This argument can be more rigorously quantified by using simple polymer physics concepts [27].

Figure 4 shows the comparison between the translocation time obtained from experiments and simulations for a wide range of applied voltage and two different polymer lengths. By fitting our results to the experimental data (with the friction coefficient fixed to its optimal value ξ_{opt} as determined above) a $\chi^2 < 1.0$ is obtained for values of q in the range $[0.35e, 0.56e]$, with an optimal value $q_{\text{opt}} = 0.4e$. An effective partial charge for DNA monomer is consistent with the mechanisms of condensation or screening that have been proposed by different studies [21,24]. The agreement is extremely good, showing an exponential dependence of the translocation time on the applied voltage, when $V_{\text{cutoff}} < V < V_{\text{crossover}}$. We can refer to the simple comparison with a chemical reaction with $\Delta F \neq 0$ to explain the observed trend. The rate constant in such a reaction is proportional to $\exp(-\Delta F/RT)$, and ΔF decreases with increasing V. Therefore, in the range $V_{\text{cutoff}} \leq V < V_{\text{crossover}}$, the translocation velocity should grow exponentially with V, as observed in our simulations. At lower V, such scaling does not hold because the translocation event is energetically unfavorable; thus, when $V < V_{\text{cutoff}}$ the translocation time quickly increases as the translocation probability drops. At higher V, the translocation event becomes energetically downhill rather than barrier crossing: this transition yields a different scaling of translocation time versus voltage.

The effect of temperature on the translocation time has been investigated experimentally only in a smaller range of T and less systematically than the dependence on L and V. However, our simple computational model is able to reproduce the experimental results correctly, as shown in Fig. 5, and clearly confirm an exponential dependence of

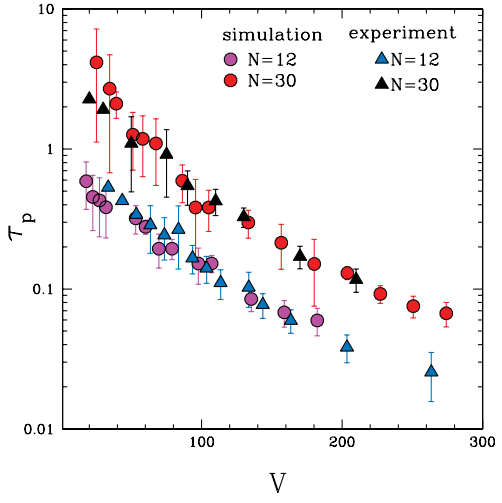

FIG. 4 (color). Dependence of τ_p with the applied potential. The experimental data correspond to poly(dA) and were extracted from Ref. [12].

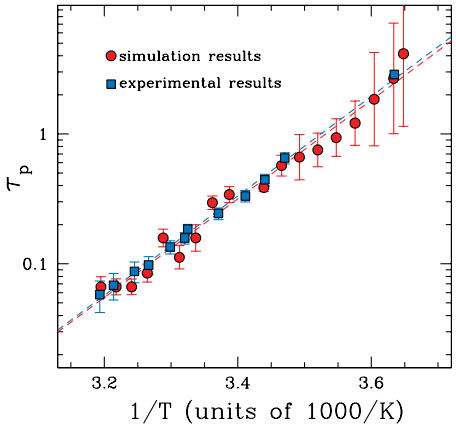

FIG. 5 (color). Dependence of τ_p with temperature for a polymer of length 100. The experimental data correspond to poly(dA) and were extracted from Ref. [5].

τ_p on T. Values of the parameter ϵ_{LJ} in the range $[0.5, 0.7]$ kcal/mol fit our results to experimental data with a $\chi^2 < 1.0$. The best fit is obtained for $\epsilon_{\mathrm{LJopt}} = 0.6$ kcal/mol ($\simeq 1RT$ at room temperature). This is consistent with the typical strength of van der Waals interactions. The experimental data have been obtained with $V = 120$ mV with $N = 100$ [12], when the translocation process is barrier crossing; therefore, the exponential dependence on the temperature can be explained theoretically once more through the chemical reaction comparison, where the reaction rate is proportional to $\exp(-\Delta F/RT)$. Simulations show quantitative agreement with the experimental results.

This Letter reports a simple, coarse-grained computational model for polymer translocation through a nanopore; for the first time, such a model can reproduce all the experimentally observed trends. Moreover, we provide a theoretical framework for explaining simulations and experimental results. The present work clearly indicates the relevant time and energy scales of the process. The actual friction coefficient inside the pore (or equivalently the coupling time τ_0) depends on the strong confinement; the equivalent unit charge of the monomer q is affected by the counter-ion distribution, and the Lennard-Jones potential between polymer and pore walls ϵ_{LJ} depends on the pore chemistry. Future work may focus on *ab initio* prediction of these three parameters.

The authors wish to thank Giovanni Fossati for his help with computer related issues and insightful discussions. Support for this project was provided in part by grants from NSF [CHE-CAREER-0349303 (C. C.), CHE-CAREER-0237105 (A. B. K.), CTS-CAREER-0134389 (M. P.)], the Robert A. Welch Foundation [Norman Hackerman grant and C-1570 (C. C.), C-1559 (A. B. K.)], and the Sloan Foundation [BR-4418 (A. B. K.)].

*Author to whom correspondence should be addressed.
Email address: cecilia@rice.edu
Phone: +1-713-348-3485
Fax: +1-713-348-5155

[1] A. Meller, J. Phys. Condens. Matter **15**, R581 (2003).
[2] J. Nakane, M. Akenson, and A. Marziali, J. Phys. Condens. Matter **15**, R1365 (2003).
[3] H. Lodish, D. Baltimore, A. Berk, S. L. Zipursky, P. Matsudaira, and J. Darnell, *Molecular Cell Biology* (W. H. Freeman and Company, New York, 1996).
[4] J. J. Kasianowicz, E. Brandin, D. Branton, and D. W. Deamer, Proc. Natl. Acad. Sci. U.S.A. **93**, 13 770 (1996).
[5] D. W. Deamer and D. Branton, Acc. Chem. Res. **35**, 817 (2002).
[6] A. Meller, L. Nivon, E. Bradin, J. Golovchenko, and D. Branton, Proc. Natl. Acad. Sci. U.S.A. **97**, 1079 (2000).
[7] A. Meller, L. Nivon, and D. Branton, Phys. Rev. Lett. **86**, 3435 (2001).
[8] S. Howorka, S. Cheley, and H. Bayley, Nat. Biotechnol. **19**, 636 (2001).
[9] S. Henrickson, M. Misakian, B. Robertson, and J. J. Kasianowicz, Phys. Rev. Lett. **85**, 3057 (2000).
[10] M. Akeson, D. Branton, J. J. Kasianowicz, E. Bradin, and D. Deamer, Biophys. J. **77**, 3227 (1999).
[11] P. K. Khulbe, M. Mansuripur, and R. Gruener, J. Appl. Phys. **97**, 104317 (2005).
[12] A. Meller and D. Branton, Electrophoresis **23**, 2583 (2002).
[13] M. Bates, M. Burns, and A. Meller, Biophys. J. **84**, 2366 (2003).
[14] W. Sung and P. Park, Phys. Rev. Lett. **77**, 783 (1996).
[15] D K. Lubensky and D. R. Nelson, Biophys. J. **77**, 1824 (1999).
[16] M. Muthukumar, J. Chem. Phys. **111**, 10 371 (1999).
[17] S. Chern, A. Cardenas, and R. Coalson, J. Chem. Phys. **115**, 7772 (2001).
[18] C. Y. Kong and M. Muthukumar, Electrophoresis **23**, 2697 (2002).
[19] H. C. Loebl, R. Randel, S. P. Goodwin, and C. C. Matthai, Phys. Rev. E **67**, 041913 (2003).
[20] E. Slonkina and A. B. Kolomeinsky, J. Chem. Phys. **118**, 7112 (2003).
[21] Y. Rabin and M. Tanaka, Phys. Rev. Lett. **94**, 148103 (2005).
[22] O. Flomenbom and J. Klafter, Biophys. J. **86**, 3576 (2004).
[23] J. Mathe, A. Aksimentiev, D. Nelson, K. Shulten, and A. Meller, Proc. Natl. Acad. Sci. U.S.A. **102**, 12 377 (2005).
[24] Y. Lansac, P. K. Maiti, and M. A. Glaser, Polymer **45**, 3099 (2004).
[25] D. A. Case, T. E. Cheatham III, T. Darden, H. Gohlke, R. Luo, K. M. Merz, Jr., A. Onufriev, C. Simmerling, B. Wang, and R. Woods, J. Comput. Chem. **26**, 1668 (2005).
[26] H. J. C. Berendsen, J. P. M. Postma, W. F. van Gunsteren, A. DiNola, and J. R. Haak, J. Chem. Phys. **81**, 3684 (1984).
[27] S. Matysiak, K. Bravaya, and C. Clementi (unpublished).
[28] B. Tinland, A. Pluen, J. Sturn, and G. Weill, Macromolecules **30**, 5763 (1997).